Chemical Engineering Journal 427 (2022) 131820

Contents lists available at ScienceDirect

Chemical Engineering Journal

journal homepage: www.elsevier.com/locate/cej

Carbon black-polydopamine-ruthenium composite as a recyclable boomerang catalyst for the oxidative cleavage of oleic acid

Sebastián Gámez [a,*], Ernesto de la Torre [b], Eric M. Gaigneaux [a]

[a] Institute of Condensed Matter and Nanosciences (IMCN), Université catholique de Louvain, Place Louis Pasteur 1. L04.01.09, 1348 Louvain-la-Neuve, Belgium
[b] Department of Extractive Metallurgy, Escuela Politécnica Nacional, Ladron de Guevera E11-253, Quito 170517, Ecuador

ARTICLE INFO

Keywords:
Boomerang catalysis
Supported catalysts
Oleic acid
Polydopamine
Oxidative cleavage

ABSTRACT

A new composite heterogeneous catalytic system is proposed for the transformation of cheap unsaturated fatty acids into value-added molecules through their oxidative cleavage. The valorization of oleic acid to azelaic and pelargonic ones (which are demanded in pharmacology) is specifically studied. The reaction is efficiently performed with a novel composite catalyst inspired from metal recovery technology, namely Ru species supported on a carbon black that was previously oxidized and then functionalized with polydopamine. Being a polymer with hydroxyl and amine groups polydopamine provides moieties acting as tweezers able to complex Ru species. A representation of this novel composite catalyst is built from its characterization by FTIR, TGA, N_2 physisorption TEM and XPS. Using $NaIO_4$ as oxidizing agent in a biphasic system at room temperature the conversion of oleic acid, and selectivity towards pelargonic and azelaic acids, reached around 95% after 3 h. The reaction mechanism is explored by UV–Vis spectrophotometry, ICP elementary analysis and NMR spectroscopy, together with recyclability and hot centrifugation tests. The occurrence of a boomerang mechanism is demonstrated. The solid catalyst is indeed recyclable at least 5 times without activity loss, but at the same time Ru species are shown performing the reaction in homogeneous phase namely in a dissolved state. Actually, polydopamine is confirmed to recover Ru species once the reaction ends, guarantying the recyclability of the catalyst. The composite catalyst therefore combines the advantages of homogeneous and heterogeneous catalysis in the investigated reaction.

1. Introduction

Since the beginning of the new millennium, oils and fats have become a novel source of raw materials for non-food applications [1,2,6]. These renewable raw substrates have been employed in several reactions related to organic synthesis, polymers and pharmaceutical applications [1-3]. Among these reactions, oxidative cleavage of unsaturated fatty acids (UFAs) arises as a promising route for the production of carbonyl compounds that are not found in nature. Oxidative cleavage consists in the rupture of carbon–carbon double bonds of UFAs [1-3].

In this work we focus on the oxidative cleavage of cheap and abundant oleic acid to pelargonic and azelaic ones, which because of their odd number of carbon at-oms and/or being a diacid are much demanded molecules in the pharmacology for skin disease treatments, but yet scarcely available in Nature [4,5]. Depending on the reaction conditions and the nature of the substrates, the oxidative cleavage of UFAs gives various products such as alcohols, ketones, aldehydes, carboxylic and dicarboxylic acids [6,7] Generally, ozonolysis is the most common method for the oxidative cleavage of various kinds of olefins. In this procedure, ozone may form a cyclic ester with the carbon–carbon double bond. After a rearrangement, the ester is broken and the two products are formed. However, ozonolysis is not recommended be-cause of the toxicity of ozone and because the process is highly energy consuming [8,9].

As alternatives, catalytic systems based on transition metals have shown to be effective in the oxidative cleavage of UFAs. Their high catalytic activity results in high conversions and yields of the desired products. Mainly, ruthenium, tungsten and osmium are the most used transition metals [10-13]. They have been employed as oxides or as complexes. Among the few works carried out so far, catalytic systems have been developed with ruthenium and tungsten, while it is important to point out that with tungsten catalysts, undesired side reactions such as epoxidation, dihydroxylation or allylic oxidation are very common [12-17].

In the specific case of ruthenium, the abovementioned side reactions

* Corresponding author.
E-mail address: sebastian.gamez@uclouvain.be (S. Gámez).

https://doi.org/10.1016/j.cej.2021.131820
Received 7 June 2021; Received in revised form 4 August 2021; Accepted 10 August 2021
Available online 14 August 2021

have not been observed. In addition, ruthenium in the form of Ru(VIII)O_4 can achieve fast conversions with high selectivity toward the desired products. The oxidative cleavage mechanism with ruthenium involves the in situ formation of Ru(VIII)O_4 after the addition of a strong oxidizing agent (e.g. sodium periodate or sodium hypochlorite) to a precursor like $RuCl_3$ or RuO_2. Then, a pericyclic reaction [3 + 2] takes place between the Ru(VIII)O_4 and the carbon–carbon double bond of the UFA [17,18] The resultant product is a cyclic perruthenate ester which is broken after its interaction with water (Scheme 1).

The UFA is transformed into a diol after the rupture of the perruthenate ester, and then the diol is cleaved by the oxidizing agent to form aldehydes. It is believed that these aldehydes can be oxidized by Ru(VIII)O_4 and give carboxylic acids. Finally, once the perruthenate ester is broken, the Ru(VIII)O_4 is reduced to Ru(VI)O_4. This last Ru species is then oxidized by the oxidizing agent keeping the oxidative cleavage reaction ongoing [17,18].

Most of the works related to this subject have focused on the oxidative cleavage of oleic acid via homogenous catalysis approach, because it is easier to obtain complete conversions in short periods of time along with high selectivity [12,18]. For instance, Zimmerman and co-workers found that the solvent system H_2O/MeCN/AcOEt in a proportion (3/2/2) along with $RuCl_3$ and $NaIO_4$ can perform completely the oxidative cleavage of oleic acid with a selectivity toward azelaic acid (AA) of 73% [18,24]. Rup and co-workers found that a non-desired product (9,10-dihydroxystearic acid) is obtained as a result of an incomplete cleavage of the perruthenate intermediate. According to the authors, ethyl acetate may retain the 9,10-dihydroxystearic acid which prevents its cleavage by the excess of oxidizing agent in the aqueous layer [18,25]. However, the main drawback of homogeneous catalysis is to recover the dissolved catalysts after the reaction, and separate them from the products that need to be washed intensively to get purified.

Heterogeneous catalysts have the potential to circumvent these issues; however, poor results in terms of conversion and selectivity have been obtained [19-23]. For example, Ho et al., immobilized Ru nanoparticles on hydroxyapatite, and performed the oxidative cleavage of several alkenes, mostly methyl oleate. Under the conditions they used, despite yields of pelargonic and azelaic acids were high (84% and 79% respectively), only 16% of conversion was achieved after 12 h due to diffusional issues and likely limited metal accessibility. Still the work of Ho and co-workers shows that Ru, in form of nanoparticles, is a promising alternative for the oxidative cleavage of alkenes that worth to be further explored [26].

Therefore, the principal aim of our work consists in the conception and application of a heterogeneous catalytic composite system for the oxidative cleavage of UFAs using ruthenium as transition metal. Carbon black was selected as support for its resistance to acidic and basic conditions. In addition, its surface chemistry can be modified by several treatments which allow to obtain functional groups with great affinity for transition metal species [27-29].

In order to improve the interaction between the support and ruthenium, carbon black was covered with polydopamine (PDA). It is known that PDA functional groups can interact with metallic ions in order to distribute them on the surface support [30-32]. For instance, Chen et al., deposited Ag nanoparticles on PDA spheres in order to catalyze the reduction of Cr(VI) to Cr(III) [33]. Bimetallic deposition of Pd and Ag on PDA was accomplished as well for the reduction of nitrophenol (pollutant) in the environment [34]. Various researches are focused to medical areas like the impregnation of gallium on PDA which in turn covered $SrTiO_3$ nanotubes. This latter was used to increase osteogenic and antimicrobial activity [35]. The key point of using PDA as a complexation material is to avoid aggregation of metallic ions by the complexation of them. By this mean, it is possible to reduce the coordination sites and increase surface area of metallic ions which drive to high catalytic activity [36].

Thus, the idea consisted in fixing Ru ions on carbon black surface using PDA as an anchoring system. This new heterogeneous catalyst was then implemented in the oxidative cleavage of oleic acid with sodium periodate ($NaIO_4$) as oxidizing agent within a biphasic solution formed by H_2O/MeCN/AcOEt.

2. Experimental procedures

2.1. Materials

Heptanoic acid (Internal standard, $C_7H_{14}O_2$, >98% GC), Nonanal (NA, $C_9H_{18}O$, >95% GC), pelargonic acid (PA, $C_9H_{18}O_2$, >98% GC),

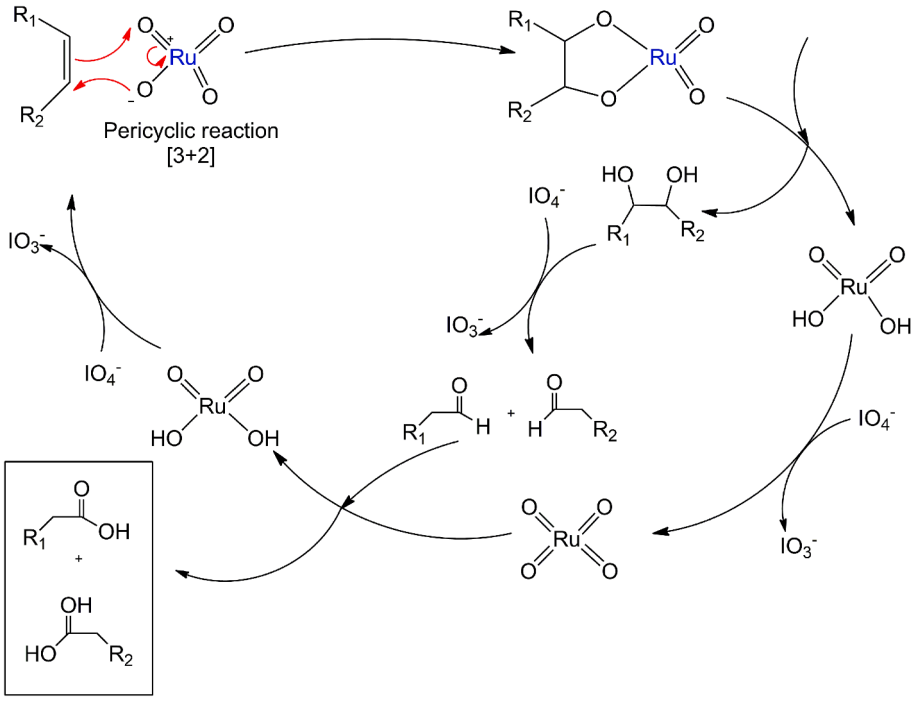

Scheme 1. Oxidative cleavage of olefins with Ru(VIII)O_4 and $NaIO_4$ (inspired from [23]).

azelaic acid (AA, $C_9H_{16}O_4$, >98% GC), tris(hydroxymethyl)aminomethane (TRIS, $C_4H_{11}NO_3$, >99.0%) and 3-hydroxytyramine hydrochloride (DA, $C_8H_{11}NO_2$, >98%), were obtained from TCI chemicals. Ruthenium(III) chloride hydrate, 99.9% (PGM basis), ($RuCl_3{\cdot}H_2O$, Ru 38%) was purchased from Alfa Aesar. Sodium metaperiodate ($NaIO_4$, >99%) was obtained from Sigma-Aldrich. Oleic acid (OA, $C_{18}H_{34}O_2$, >99.9% GC), Acetonitrile (MeCN, C_2H_3N > 99.98% GC), nitric acid (HNO_3 > 65%) and ethyl acetate (AcOEt, $C_4H_8O_2$ > 99.9% GC) were purchased from Carl Roth. 9-oxononanoic acid (Oxo, $C_9H_{16}O_3$, 95%) and 9,10-dihydroxystearic acid (diol, $C_{18}H_{36}O_4$, 95%), were obtained from abcr GmbH. Deuterated chloroform (99.8%), deuterated acetonitrile (99.9%) and deuterium oxide (99.9%) were obtained from Eurisotop. Potassium bromide for spectroscopy (≥99%) was obtained from Acros Organics. Carbon black (CB) was purchased from Degussa (specific surface area 154 m^2/g and pore volume 0.76 cm^3/g).

2.2. Preparation of CBO-PDA-Ru

First, 10 g of carbon black (CB) were added to a 5.0 M HNO_3 solution at 80 °C. The black suspension was stirred for 8 h under reflux. Afterwards, the solid was removed by centrifugation at 14 000 rpm (26 200 g) in a Heraeus MultifugeX1R Centrifuge, washed with warm distilled water until water pH arrived to 6.5. Then, the solid was dried in air at 110 °C overnight [37]. For the impregnation of PDA on CBO surface, 100 mL of a 10 mM buffer solution of TRIS was prepared in an open vessel and stirred for 15 min. Afterwards, 200 mg DA was dissolved in the buffer solution at a pH of 8.5. Dopamine started to self-polymerize when the solution passed from colorless to pale brown. At this moment, 1 g of dried CBO was added to the solution and stirred for 24 h at room temperature in order to ensure a complete deposition of PDA on the support. Next, the CBO-PDA composite was removed by centrifugation, washed 3 times with distilled water and dried overnight at room temperature (see Scheme 2) [32,38].

500 mg of CBO-PDA was added into 20 mL of distilled water in order to disperse the particles by ultrasonic treatment for 15 min. Afterwards, 10 mL of $RuCl_3{\cdot}H_2O$ solution (10 mM) was added to the above solution, and then stirred for 24 h. The amount of ruthenium was varied in order to obtain Ru loads of 1%, 2% and 4% on the composite. Then, the solid was separated from the solution by centrifugation at 14 000 rpm for 20 min. The solid catalyst was washed with distilled water 3 times, and dried at room temperature [39,40].

2.3. Polydopamine synthesis

As a reference material, pure polydopamine was prepared. First, 0.24 g of tris(hydroxymethyl)aminomethane (TRIS) were dissolved in 200 mL of distilled water (10 mM) and stirred for 15 min. Then, 1.00 g of 3-hydroxytyramine hydrochloride (DA) was dissolved in the TRIS solution at a pH of 8.5. At the beginning the solution is transparent, then it turns pink and finally it becomes dark brown which means that dopamine self-polymerized. The solution was stirred for 24 h at room temperature to allow a complete polymerization of PDA. Afterwards, PDA particles were separated by centrifugation, washed 3 times with distilled water and dried overnight at room temperature [41].

2.4. Characterization

The morphology of carbon black (CB) as well as particle size distribution before and after polydopamine (PDA) deposition was determined by transmission electron microscopy (TEM) in a LEO 922 microscope with an acceleration voltage of 200 kV and equipped with a LaB6 thermal cathode. From each image, the diameter of 25 particles were measured in order to obtain the mean particle size and the standard deviation from a frequency distribution graphic (histogram). The influence of PDA on CB textural properties were determined by N_2 physisorption at −196 °C in a Micromeritics Tristar 3000 equipment. Before the analysis, 50 mg of sample was degassed overnight under vacuum (~10.7 Pa) at 150 °C. The total surface area was calculated by the Brunauer-Emmet-Teller (BET) method using the adsorption isotherm in the partial pressure range from 0.05 to 0.30. Pore volume and pore size

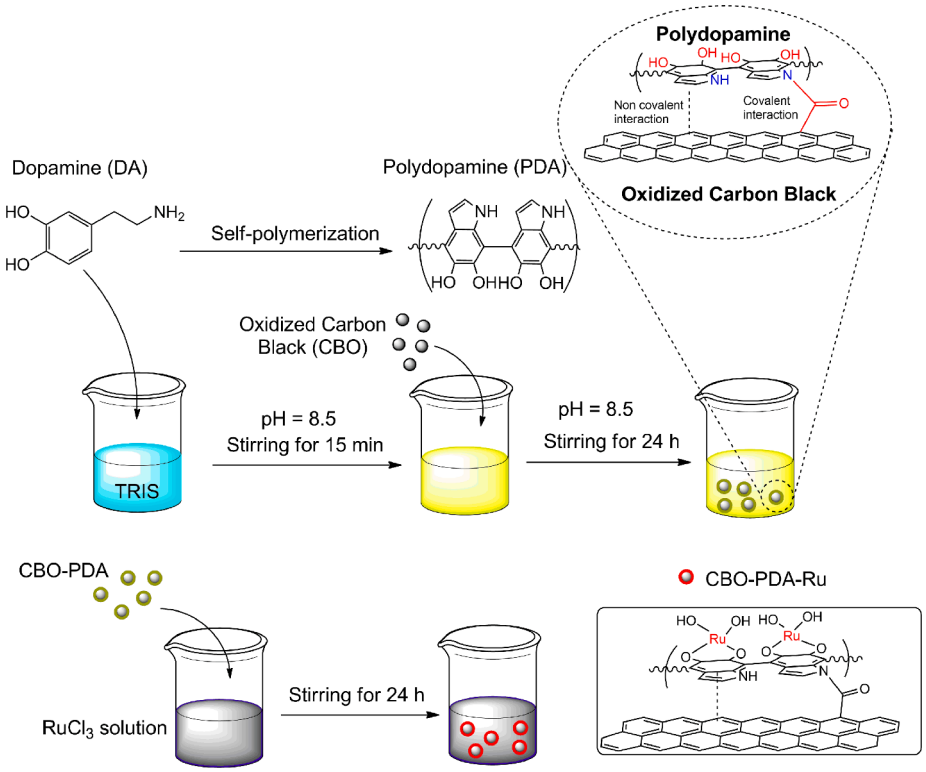

Scheme 2. Preparation of Ru heterogeneous catalyst based on oxidized carbon black with polydopamine (CBO-PDA-Ru).

distribution were estimated by Barrett, Joyner and Halenda method (BJH) using the data from the desorption isotherm branch [42].

Infrared spectroscopy was performed to identify the characteristic peaks of PDA deposited on the support. For this purpose, wafers were prepared by mixing 15 mg of sample with 300 mg of KBr beforehand dried overnight at 110 °C. All analyses were carried out in a Perkin Elmer equipment Spectrum One. One hundred scans were carried out in the range of 4000 to 400 cm^{-1} with a 4 cm^{-1} resolution. Thermogravimetric analysis was employed to determine the amount of PDA deposited on carbon surface. All tests were carried out under a nitrogen atmosphere from 50 °C to 900 °C in a Perkin Elmer STA 8000 thermobalance. The heating ramp was kept at 10 °C/min and the N_2 flow rate was adjusted to 40 mL/min. With this technique it was possible to calculate the amount of PDA deposited on carbon black surface by estimating the difference in the weight loss during the heating process.

The amount of functional groups on CBO-PDA composite was determined by Boehm's titration. Samples were put in contact with 50 mL of 0.05 M solutions of NaOH, Na_2CO_3 and $NaHCO_3$ under magnetic stirring and nitrogen atmosphere. After filtrating the solid, 10 mL of each sample was acidified with 20 mL of 0.05 M HCl solution. The new solutions were degassed for 2 more hours with nitrogen under agitation and titrated with 0.05 M NaOH in order to determine the amount of phenols, lactones and carboxylic groups [43,44].

Ruthenium load on each composite was measured by ICP-AES in a ICP 6500 Thermo Scientific Instrument. For this matter, samples were mixed with 1 g of NaOH and Na_2O_2 and melted on the flame of a Bunsen burner. The samples were analyzed after they were acidified with HCl and diluted with distilled water. Ruthenium dispersion was measured by CO chemisorption in a Micromeritics PulseChemiSorb 2705. For this latter, samples of 0.25 g were reduced at 200 °C for 2 h under hydrogen atmosphere (Air liquid; Purity > 99.999%) with a heat ramp of 10 °C/min. After reduction, helium (Air liquid; Purity > 99.999%) was passed through for 1 h until the temperature decreased to 35 °C. Under these conditions, CO pulses (20% of CO in Helium as carrier gas) were introduced. A TCD detector was employed to estimate the CO moles not adsorbed by Ru and thereafter to estimate Ru dispersion. Under the analysis conditions, metallic ruthenium on the surface adsorbs CO molecules with a stoichiometric ratio of Ru:CO = 1:1 [45].

X-ray photoelectron spectroscopy (XPS) analyses were carried out in a SSX 100/206 photoelectron spectrometer from Surface Science Instruments (USA) equipped with a monochromatized micro focused Al X-ray source (powered at 20 mA and 10 kV). The pressure in the analysis chamber was around 10–6 Pa and the flood gun was set at 8 eV. The angle between the surface and the axis of the analyzer lens was 55°. The analyzed area was approximately 1.4 mm2 and the pass energy was set at 150 eV. Under these conditions, the full width measured at half maximum (FWHM) of the Au $4f_{7/2}$ peak for a clean gold standard sample was about 1.6 eV. Samples were prepared by pressing the powder in small stainless steel troughs of 4 mm diameter and placed on a ceramic carousel with a Ni grid set above the sample surface for charge stabilization. The following sequence of spectra was recorded: survey spectrum, C 1 s, O 1 s, N 1 s, Cl 2p, Ru 3p. For all samples, C 1 s spectrum was recorded again to check the stability of charge compensation with time. The aromatic C-(C,H) component of the C1s peak of carbon was fixed at 284.8 eV to set the binding energy scale. Data treatment was performed with the CasaXPS program (Casa Software Ltd, UK). Carbon 1 s peaks were decomposed with the least squares fitting routine provided by the software with a Gaussian/Lorentzian (85/15) product function and after subtraction of a non-linear baseline. The identification and quantification of Ru was performed with the $3p_{3/2}$ peak in order to avoid deconvolution problems associated with the C 1 s peak (C 1 s and Ru $3d_{5/2}$ peaks have similar binding energies) [46]. XPS was employed to verify Ru chemical environment after PDA deposition on CBO and to estimate Ru oxidation state on catalyst surface.

2.5. Catalytic tests

All tests were carried out in 20 mL closed vessels with magnetic agitation at room temperature. Two different amounts of $NaIO_4$ were tested in this study: 4.1 equivalents (430 mg) and 8.2 equivalents (870 mg). The oxidant was dissolved in 8 mL of distilled water followed by 4 mL of acetonitrile and 2 mL of ethyl acetate. Next, 1 equivalent (0.5 mmol) of oleic acid along with heptanoic acid (internal standard) was dissolved in the biphasic solvent system. After adding 0.1 g of CBO-PDA-Ru, the reaction mixture was agitated at 1 500 rpm for 24 h (see Scheme 3).

At different time intervals, 0.1 mL of the organic layer was extracted through a syringe and diluted in 1.4 mL of ethyl acetate. All samples were analyzed by Gas Chromatography (GC) in order to separate, identify and quantify the reaction products and unreacted oleic acid. The analyses of each sample were performed in a Varian 3800 Gas Chromatograph equipped with a Flame Ionization Detector (FID). In this study, a Stabilwax-DA Restek column, formed by a crossbond acid-deactivated Carbowax polyethylene glycol as stationary phase, was employed in order to inject directly the samples from the organic layer without performing any derivatization process. Once an oxidative cleavage test ended, three subsequent extractions from the aqueous phase were performed with ethyl acetate in order to recover all the pelargonic and azelaic acids that could have formed an emulsion. The yields reported in the following are calculated by summing the quantities of PA and AA found in the reaction organic phase with those found in the three extracts from the aqueous phase.

Isolated yield was obtained as well by separating pelargonic and azelaic acids employing Rup et al., protocol [18]. Once the products are isolated in ethyl acetate after three extractions, the acids were concentrated using a rotary evaporator at 50 °C. The paste obtained was purified twice with hot distilled water (90 °C) in order to dissolve azelaic acid. Pelargonic acid, which is not soluble in water, was dissolved in petroleum ether, stirred for 2 h and dried in order to obtain the product. Azelaic acid precipitated once hot water reached room temperature.

In addition, oxidative cleavage of oleic acid with CBO-PDA-Ru was monitored by UV–Vis spectrophotometry in a UV-3600 Plus Shimadzu spectrophotometer. Samples from the aqueous and organic phases were extracted separately at different time intervals in order to verify the presence of Ru species in both phases during the reaction and after it was concluded. In the case of the aqueous phase, a solution of $NaIO_4$ was used as reference; ethyl acetate was used as reference for the organic phase.

The same procedure was performed with deuterated solvents (D_2O, acetonitrile-d_3 and $CDCl_3$) in order to verify the intermediates and products throughout the oxidative cleavage of oleic acid with CBO-PDA-Ru composites. At the same interval times, samples were extracted from the organic phase to analyze them in a Liquid-state Nuclear Magnetic Resonance (NMR) spectroscopy Bruker Avance II 300 MHz equipped with a BBFO 5 mm NMR probe z-gradient coil. For each experiment 16 scans were recorded; the spectral window was set at 16 ppm with a relaxation delay of 3 s. All data was treated with Spinwork 4 software.

2.6. Recyclability tests

Once a catalytic test was finished, the catalyst was separated from the biphasic solution by centrifugation in a Heraeus MultifugeX1R Centrifuge at 14 000 rpm (26 200 g) for 20 min. The solid catalyst was washed three times with warm distilled water (~80 °C) and dried overnight at room temperature. Afterwards, the catalyst was re-inserted in a fresh reaction mixture to start the oxidative cleavage of oleic acid with the procedure explained above. These steps were repeated five times in order to verify the possibility of re-use the synthesized catalyst by assessing conversion after each recycle test.

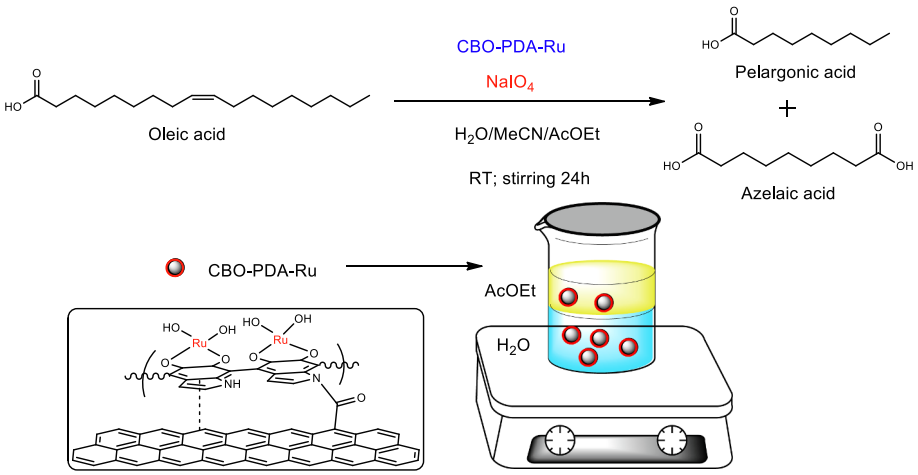

Scheme 3. Oxidative cleavage of oleic acid with Ru catalyst and $NaIO_4$.

2.7. Hot-centrifugation tests

In these tests, once the conversion in a standard test described above was approximately 50%, the catalyst was removed from the reaction medium by centrifugation. Then, the reaction continued to be monitored (without the solid catalyst) by injecting samples of the organic layer in the chromatograph. The idea was to verify if there was catalytic activity after the removal of the solid catalyst. An increase in conversion after the catalyst removal would suggest that the active sites (ruthenium species) have moved in the liquid phase leaving the composite and were exerting a catalytic effect therein.

2.8. Boomerang catalysis assessment protocol

The possibility that Ru ions could be released from the CBO-PDA support and return to it once the oxidative cleavage reaction ended, was verified by following the protocol depicted in Fig. 1. After an oxidative cleavage test finished, the solid catalyst was removed by centrifugation. The organic phase was separated from the aqueous layer by a syringe. Then, a fresh support (CBO-PDA) was added to the aqueous phase in order to adsorb the eventually leached Ru ions from the original solid catalyst. After 24 h of adsorption, the solid was removed from the aqueous solution by centrifugation. The aqueous phase before and after adsorption was analyzed by ICP to determine the presence of Ru ions. Finally, both the CBO-PDA that has been used to recover the eventually leached Ru, and the aqueous layer were respectively submitted to one more oxidative cleavage test.

3. Results and discussion

Characterization of synthesized CBO-PDA-Ru catalyst TEM images (Fig. 2) demonstrate that oxidized carbon black (CBO) appears as aggregates of particles with average particle size of 27.8 ± 10.7 nm. On the other hand, PDA appears as a layer that covers CBO nanoparticles, increasing their average particle size to 41.2 ± 7.3 nm.

All carbonaceous composites showed a quasi-type 2 isotherm with a narrow hysteresis loop H3 which is characteristic of materials displaying big mesopores (Fig. S1). In the case of the CBO-PDA composite, the specific surface area diminished as compared to CBO from 154 to 80 m^2/g. The pore volume also decreased by a factor 2, due to the filling of the gaps in between particles by the PDA. Comparatively, CBO specific surface area and pore volume only slightly decreased after Ru impregnation (Table S1).

FTIR analysis was carried out to verify PDA deposition on oxidized

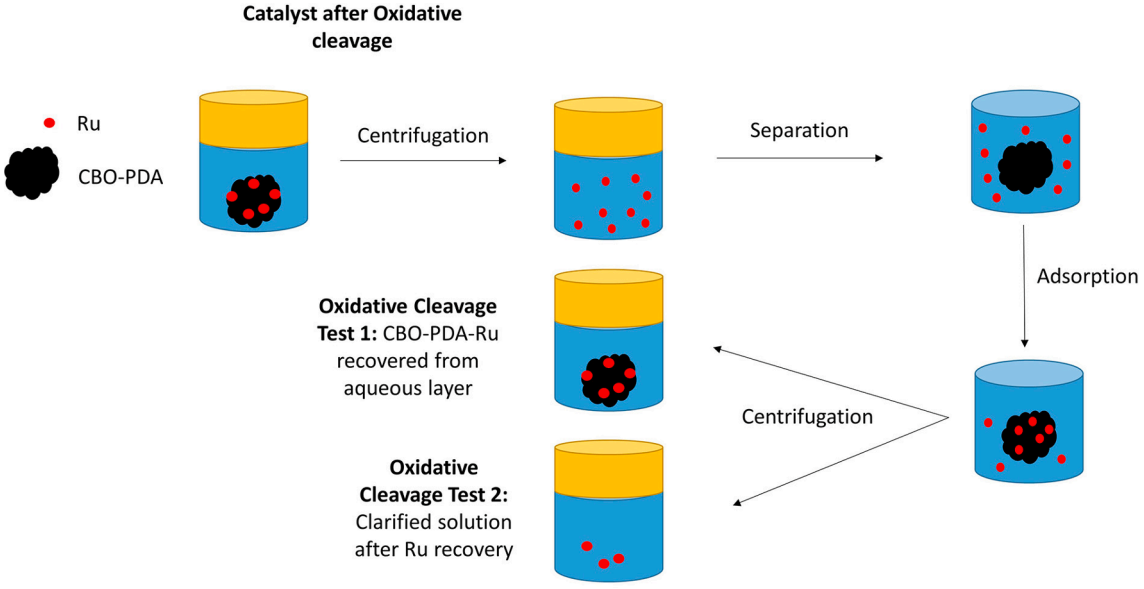

Fig. 1. Boomerang catalysis assessment protocol.

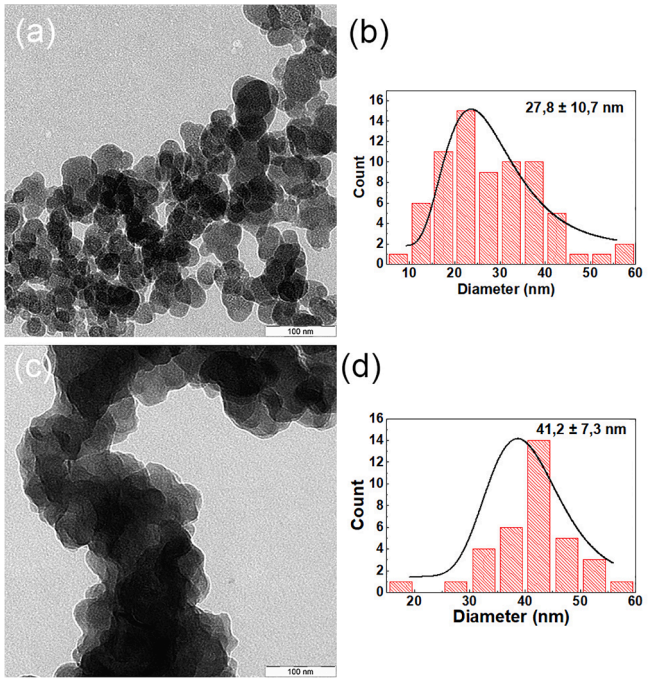

Fig. 2. TEM images of a) CBO; b) particle size distribution of CBO; c) CBO-PDA; d) particle size distribution of CBO-PDA.

carbon black (Fig. S3). After PDA deposition on CBO, the characteristic peaks of PDA appear at 1604 and 1502 cm^{-1} which correspond to the stretching vibration modes of the N–H bond located in the indole ring. The broad peak at 3446 cm^{-1} and a small peak at 1263 cm^{-1} are also observed which corroborates the presence of the polymer on the oxidized carbon black aggregates [38,40,41]. Therefore, it is possible to affirm that PDA was successfully deposited on oxidized carbon black nodules.

Boehm's titration results in Table S2 demonstrated that the amount of phenol groups increased from 0.04 to 0.18 mmol/g after PDA deposition. The amount of phenol groups available on CBO-PDA surface is in principle higher than the amount of Ru atoms required to obtain a load of 4%, and more than enough to chelate Ru atoms corresponding to Ru loads of 1% and 2%.

As regard to TGA, the amount of PDA was possible to determine by subtracting the weight loss of CBO from the weight loss of CBO-PDA composite. In this latter, the additional weight loss observed is attributed to the thermal decomposition of PDA (Fig. S3). From 50 °C to 250 °C, humidity is evaporated and then PDA starts to decompose through the entire range of temperature up to 900 °C. Thus, a 15% PDA content on CBO surface was estimated.

After ruthenium impregnation on CBO and CBO-PDA, Ru loading and dispersion on each composite were measured. The wet impregnation method was efficient in Ru deposition since ICP results agreed with the nominal values (Table 1).

As regards CO chemisorption results, PDA apparently induced a marked decrease of Ru dispersion on the sup-port. However, this could be related to the chelation of Ru atoms by functional groups of PDA, as if Ru atoms are interacting with catechol groups it is less probable that CO could form a covalent bond with Ru during chemisorption analysis, thus the apparent decrease of Ru dispersion. Therefore, the values reported in Table 1 may correspond to only Ru ions that did not form a complex with PDA, and formed clusters on CBO surface instead.

Table 1
Ru loading and dispersion on carbon black composites.

Catalyst	Ru loading (Nominal value) (%)	Ru loading (ICP value) (%)	Ru dispersion (%)
CBO-Ru(2%)	2.0	1.7	47.8
CBO-PDA-Ru (1%)	1.0	1.0	8.4
CBO-PDA-Ru (2%)	2.0	1.9	7.8
CBO-PDA-Ru (4%)	4.0	3.8	4.8

By TEM analysis (Fig. 3) of CBO-PDA-Ru (2%), it was very difficult to visualize Ru nanoparticles on CBO-PDA surface which might suggest that there was not Ru at all. However, since ICP confirmed the presence of Ru on each synthesized composite, it can be concluded that Ru is ideally dispersed, presumably atomically bonded to functional groups of PDA. On this basis, CO chemisorption results must thus be understood as telling that a main part of the nominal Ru is effectively complexed by PDA as desired.

X-ray photoelectron spectroscopy (XPS) spectra were performed to estimate the chemical composition of PDA and the oxidation state of Ru on the synthesized composites. For PDA (Fig. S5a), the presence of C, N and O was observed. In addition, the peak corresponding to C 1 s was decomposed. Four contributions were found corresponding to CH-CH bonds (284.8 eV), C-N bonds in the aromatic ring (286.3 eV), C-OH of catechol groups (288.4) and a shake-up peak at 290.1 eV which is characteristic of aromatic structures ($\pi \rightarrow \pi^*$) (Fig. S4c) [36,37].

The same peaks were observed for PDA-Ru (Fig. S4b and Fig. S4d) with the addition of Ru 3p and 5d peaks. The Ru 3p doublet (Fig. S4e) was employed to estimate the oxidation state of Ru on PDA. Therefore, Ru $3p_{3/2}$ and Ru $3p_{1/2}$ were decomposed into four sub-peaks. The contributions at 463.0 eV and 485.2 eV could be interpreted as Ru(IV), while those at 466.1 eV and 488.5 eV are satellite peaks of the former [47-50].

As regards CBO (Fig. 4a), C 1 s and O 1 s appear at 284.8 eV and 532.8 eV respectively, and the presence of N was confirmed by the N 1 s peak at 400.0 eV in the CBO-PDA spectrum (Fig. 4b). The presence of nitro-gen along with the increase of oxygen content (because of catechol groups) confirms the deposition of PDA on CBO surface.

Table 2 recaps the elemental composition of the analyzed samples. The presence of nitrogen in CBO-Ru (2%) could be due to the presence of impurities while the presence of Cl can be attributed to the nature of the Ru precursor salt ($RuCl_3 \cdot H_2O$).

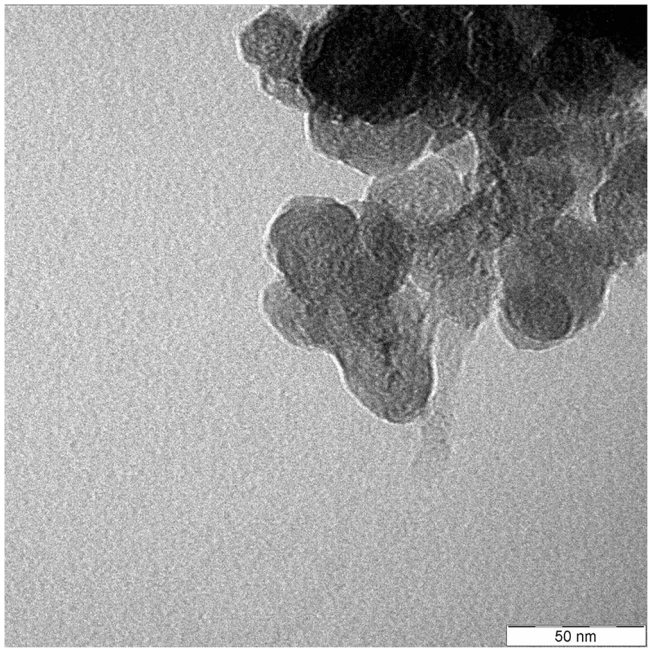

Fig. 3. TEM image of CBO-PDA-Ru (2%).

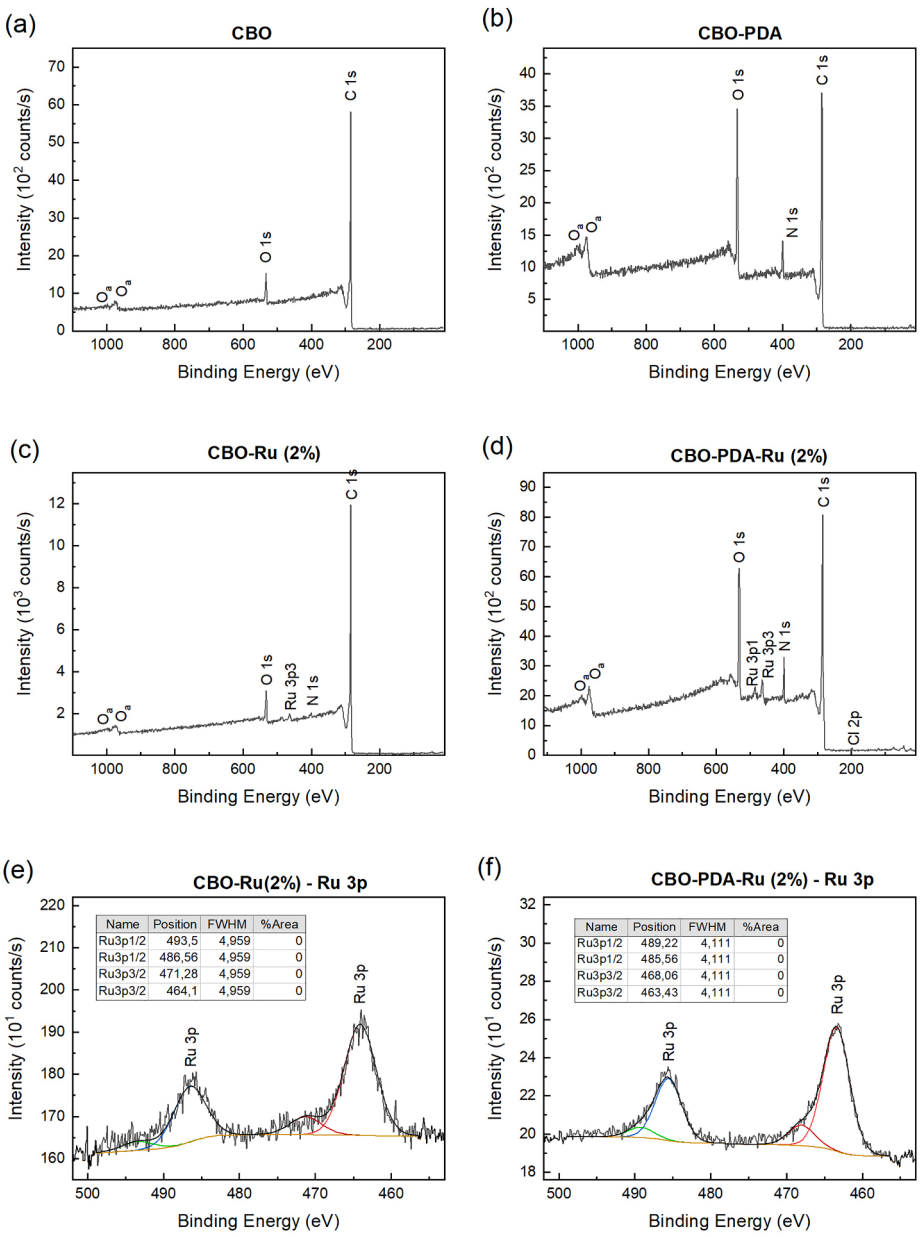

Fig. 4. XPS spectra of: (a) CBO; (b) CBO-PDA; (c) CBO-Ru (2%); (d) CBO-PDA-Ru (2%); (e) Ru(3p) core level of CBO-Ru (2%); (f) Ru(3p) core level of CBO-PDA-Ru (2%).

Table 2
Superficial chemical composition (from XPS) of carbon black composites.

Catalyst	C (%)	O (%)	N (%)	Ru (%)	Cl (%)
CBO	93.6	6.4	—	—	—
CBO-PDA	70.8	22.4	6.8	—	—
CBO-Ru (2%)	89.6	8.0	1.4	0.8	0.1
CBO-PDA-Ru (2%)	68.8	21.6	7.7	1.7	0.3

For CBO-Ru (2%) and CBO-PDA-Ru (2%), the doublet peaks of the Ru 3p core level was observed. In the case of CBO-Ru (2%), the Ru 3p doublet at 464.1 eV and 486.6 eV corresponds to Ru (III) while in CBO-PDA-Ru (2%) peaks at 463.4 eV and 485.6 eV correspond to Ru (IV) [35,38]. Therefore, the conclusion is that Ru forms a complex with PDA functional groups on CBO-PDA surface.

3.1. Elucidating oxidative cleavage mechanism of oleic acid with CBO-PDA-Ru

First, the oxidative cleavage of oleic acid was carried out only with $NaIO_4$ (entry 1, Table 2) in order to determine to what extent the oxidant agent could perform the reaction by itself without catalyst. Then, the same catalytic tests were performed with CBO, PDA and CBO-PDA (entries 2, 3 and 4, Table 3) to evaluate the possibility of oxidative cleavage without ruthenium. Conversions resulted to be lower than 1% and the products did not appear on the chromatograms. This demonstrates that it is not possible to perform the reaction with only the oxidant agent and the supports, i.e. without catalyst.

Afterwards, CBO-Ru (2%) was assessed in the oxidative cleavage reaction but with hydrogen peroxide in-stead of $NaIO_4$. The idea was to probe if it was possible to perform the reaction with a softer oxidant since ac-cording XPS results, Ru was already oxidized. However, results were as poor as in the previous cases (entry 5, Table 3). This is in line with the fact that only a strong oxidant agent such as $NaIO_4$, can

Table 3
Catalytic test results for carbon black catalysts.[a]

Entry	Catalyst	Conversion (%)	OA (%)	PA (%)	AA (%)	NA (%)	Oxo (%)	Diol (%)
1	Blank	0.5	—	—	—	—	—	—
2	CBO	0.4	—	—	—	—	—	—
3	PDA	0.6	—	—	—	—	—	—
4	CBO-PDA	0.7	—	—	——	—	—	—
5	CBO-Ru(2%)[b]	0.4	—	—	—	—	—	—
6	CBO-Ru(2%)	95.5	2.8	40.0	39.8	8.5	8.2	0.8
7	CBO-PDA-Ru(2%)	96.4	2.0	48.1	48.7	—	—	1.2

[a] All experiments were performed with: 0.5 mmol of Oleic acid, 8.2 eq (870 mg) $NaIO_4$, 8 mL H_2O, 4 mL Acetonitrile, 2 mL Ethyl Acetate and 0.1 g of catalyst (2% Ru) at room temperature during 24 h of agitation.
[b] CBO-Ru (2%) with 3 mL of H_2O_2 instead of $NaIO_4$.

transform the ruthenium precursor into $Ru(VIII)O_4$ whereas softer oxidants (as H_2O_2) cannot produce this active species [13,18,24,51].

It is important to mention that Ru at high oxidation state is required to trigger the pericyclic reaction with the carbon–carbon double bond of oleic acid. After the addition of $NaIO_4$ to CBO-Ru (2%) and CBO-PDA-Ru (2%), conversions increased to 95.5% and 96.4% respectively (entries 6 and 7, Table 3). About selectivities to PA and AA, it is important to remind that the cleavage of oleic acid should generate equal amounts of pelargonic and azelaic acids (50:50). Selectivities of PA and AA resulted to be higher with the catalysts that contain PDA.

Isolated yields of pelargonic and azelaic acids are reported in Table 4. Results demonstrate that both catalyst are efficient towards the production of carboxylic and dicarboxylic acids from oleic acid. The results obtained in this work are similar to those reported by Rup et al. [18] (88% PA and 78% AA; homogeneous catalysis), and better than those obtained by Ho and co-workers [26] (conversion 16%, 84% PA and 79% AA; heterogeneous catalysis).

In addition, three more products were detected during the oxidative cleavage tests (Figs. S5 and S6a). At the end of catalytic tests with CBO-Ru (2%) and CBO-PDA-Ru (2%), nonanal (NA, namely the aldehyde of PA), 9-oxononanoic acid (Oxo, namely the aldehyde of AA) and 9,10-dihydroxystearic acid (Diol, namely the corresponding diol of oleic acid) were additionally detected which agrees with the reaction mechanism explained in Scheme 1. The selectivities to each of them were respectively 8.5, 8.2 and 0.8 % when CBO-Ru (2%) was used as catalyst.

In the case of CBO-PDA-Ru (2%), nonanal and 9-oxononanoic acid were not detected after 24 h of agitation. On the other hand, only 1.2% of 9,10-dihydroxystearic acid was found. Fig. S5 illustrates the chromatogram with the peaks of all products involved in this reaction. In addition, all products were characterized by Nuclear magnetic resonance spectroscopy (Figs. S7–S12). In order to better understand the behavior of the system, the kinetics of the oxidative cleavage of oleic acid was then monitored with CBO-PDA-Ru (2%) at different time intervals (Fig. S6a). After 3 h of agitation, the presence of the aldehydes and the diol in the reaction medium was confirmed. At the fifth hour, aldehydes concentration reaches its maxi-mum and then their concentration started to decrease. The same trend was observed for 9,10-dihydroxystearic acid but in lower concentration than the aldehydes. At 24 h, pelargonic and azelaic acids are the most abundant products while oleic acid along with the aldehydes and 9,10-dihydroxystearic acid were found in lower concentrations in the reaction medium. These findings confirm that 9,10-dihydroxystearic acid is formed when the perruthenate ester is broken. As a result, two aldehydes (nonanal and 9-oxononanoic acid) are formed, which in turn are transformed into carboxylic acids either by means of $NaIO_4$ or by $Ru(VIII)O_4$.

In order to elucidate which one of the above oxidants may oxidize the aldehydes, the following experiment was performed. First, 0.5 mmol of nonanal was dis-solved in the absence of any Ru species in the biphasic system along with 430 mg of $NaIO_4$. Second, the same procedure was performed but in this case 5 mg of $RuCl_3{\cdot}H_2O$ was added in order to form $Ru(VIII)O_4$ in the reaction medium. The results plotted in Fig. 5 demonstrate that both $NaIO_4$ and $Ru(VIII)O_4$ can oxidize aldehydes to carboxylic acids under the same conditions of oxidative cleavage.

A difference is however observed in the kinetics of the respective oxidizing agents. While $Ru(VIII)O_4$ completely oxidizes nonanal in 5 h, $NaIO_4$ requires more time, with 24 h not being enough to completely oxidize nonanal.

Additionally, UV–Vis analysis of the evolution of the Ru oxidation state along the reaction was performed. Fig. 6 shows UV–Vis spectra of the organic (ethyl acetate) and aqueous phases after 3 h and 24 h of agitation. At three hours, three defined peaks at 295, 375 and 455 nm were observed. According to literature, $Ru(VIII)O_4$ characteristic peaks are at 300 and 380 nm whereas peaks at 380 and 455 nm correspond to $Ru(VI)O_4$ [40]. Therefore, both Ru species are present during the oxidative cleavage tests. $Ru(VIII)O_4$ performs the pericyclic reaction in first, and after the perruthenate ester is bro-ken, the Ru species is reduced to $Ru(VI)O_4$. Then, $Ru(VI)O_4$ is oxidized again by means of $NaIO_4$.

In addition, at 24 h all the characteristic peaks disappear indicating that Ru species were no longer pre-sent in the organic phase. In the aqueous phase, it is possible to observe a small peak at 325 nm at 3 and 24 h of agitation. This peak is characteristic of $RuCl_3$ which may be present in the aqueous phase when it is reduced from the oxidative cleavage in the organic phase. In the aqueous phase, no Ru at high oxidation state was never detected. These results suggest that Ru(IV) is released from the CBO-PDA support once the oxidative cleavage

Table 4
Isolated yield of pelargonic and azelaic acids.

Entry	Catalyst	Conversion (%)	Isolated Yield	
			Pelargonic acid (%)	Azelaic acid (%)
1	CBO-Ru(2%)	> 99	84.5	78.3
2	CBO-PDA-Ru (2%)	> 99	88.7	84.2

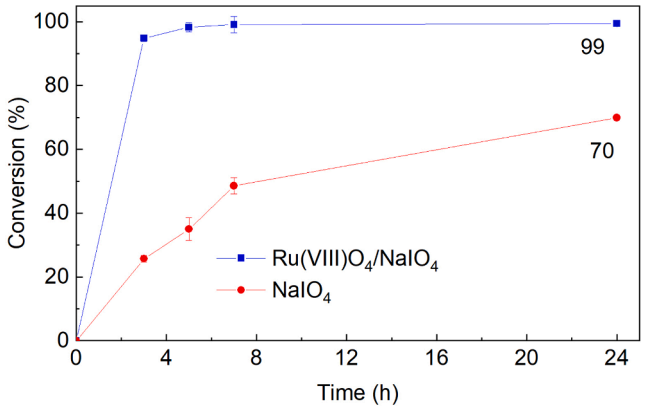

Fig. 5. Oxidation of nonanal with $NaIO_4$ and $Ru(VIII)O_4/NaIO_4$.

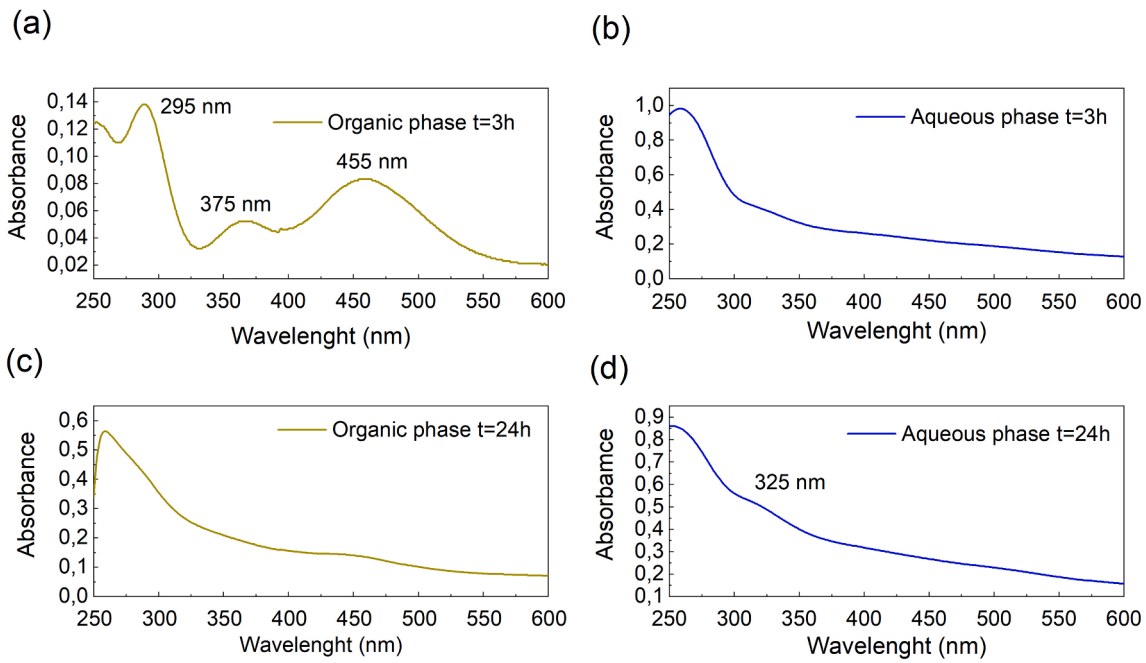

Fig. 6. Oxidative cleavage reaction with CBO-PDA-Ru (2%) monitored by UV–Vis spectrophotometry: a) Organic phase at t = 3 h, b) aqueous phase at t = 3 h, c) Organic phase at t = 24 h, b) aqueous phase at t = 24 h.

reaction begins. Then Ru is oxidized by $NaIO_4$ and performs the oxidative cleavage as a homogeneous catalyst.

3.2. *CBO-PDA-Ru towards oxidative cleavage of oleic acid*

A kinetic study was carried out during 24 h in order to determine the required time to reach the highest conversion with the synthesized catalysts. Fig. 7a demonstrates that at the first 7 h, the reaction proceeds faster than the next 17 h. In the specific case of CBO-Ru (2%), 24 h are required to achieve 95.5% conversion with 870 mg of $NaIO_4$ whereas about the same conversion (96.4%) was accomplished in no>8 h when CBO-PDA-Ru (2%) was employed as catalyst. About the selectivity, comparing CBO-PDA-Ru (2%) and CBO-Ru (2%), the presence of PDA on the support led to increase the amount of pelargonic and azelaic acids. From this comparison, the interaction between PDA functional groups and Ru turns not to be detrimental for the oxidative cleavage of oleic acid, on the contrary.

Next, the influence of higher Ru loads on CBO-PDA support along with 870 mg of $NaIO_4$ was assessed on the conversion and selectivity in the oxidative cleavage of oleic acid. Fig. 8a indicates that the higher the quantity of Ru on catalyst surface, the higher is the con-version. Fig. 8b demonstrates that not>3 h is required to obtain a complete conversion when CBO-PDA-Ru (4%) is employed.

On the other hand, both conversion and selectivity resulted to be poor with the CBO-PDA-Ru (1%) composite. Although conversion was 95%, after 24 h of agitation, there was still 9-oxo nonanoic acid and nonanal present in the reaction medium. Therefore, the selectivities towards PA and AA were lower compared to that obtained with the composites with higher Ru loads. Even an excess of 870 mg of $NaIO_4$ was not enough to oxidize the corresponding aldehydes to pelargonic and azelaic acids. In terms of selectivity, the best compo-sites resulted to be with 2% and 4% of Ru load.

Recyclability tests were performed with CBO-Ru (2%) and CBO-PDA-Ru (2%) catalysts in order to verify their reusability. CBO-Ru (2%) maintained the same catalytic activity after 2 recycles (Fig. 9a). Nevertheless, con-versions decreased ostensibly at the 3rd, 4th and 5th recycle, which suggests that CBO-Ru loses Ru in the reaction medium. On the contrary, conversions plotted in Fig. 9b demonstrate that CBO-PDA-Ru (2%) can be re-used without major loss of catalytic activity even after 5 recycles.

Only in the last two recycles, at the first 7 h of the reaction the catalytic activity of the composite was slightly lower than in the three first runs. The reason can be the progressive physical loss of support (and therefore also of Ru) accumulating at each recyclability test or during

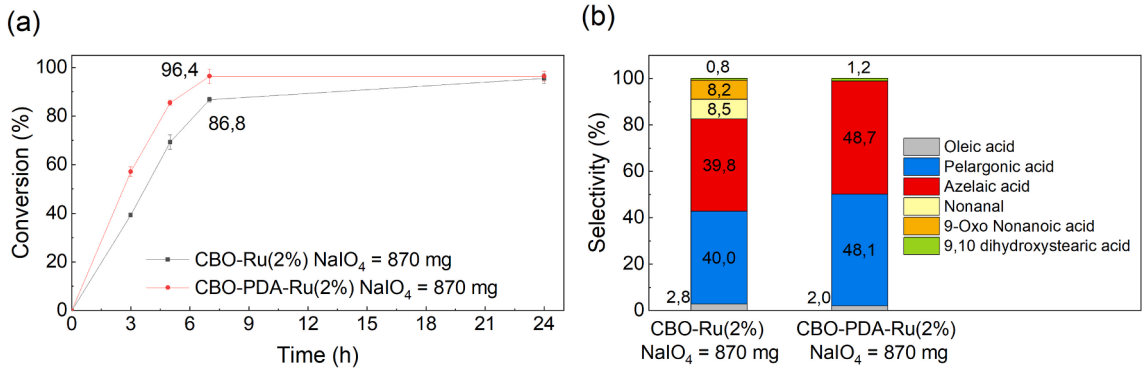

Fig. 7. a) Kinetics of CBO-Ru (2%) and CBO-PDA-Ru (2%); b) Selectivity of CBO-Ru (2%) with different amounts.

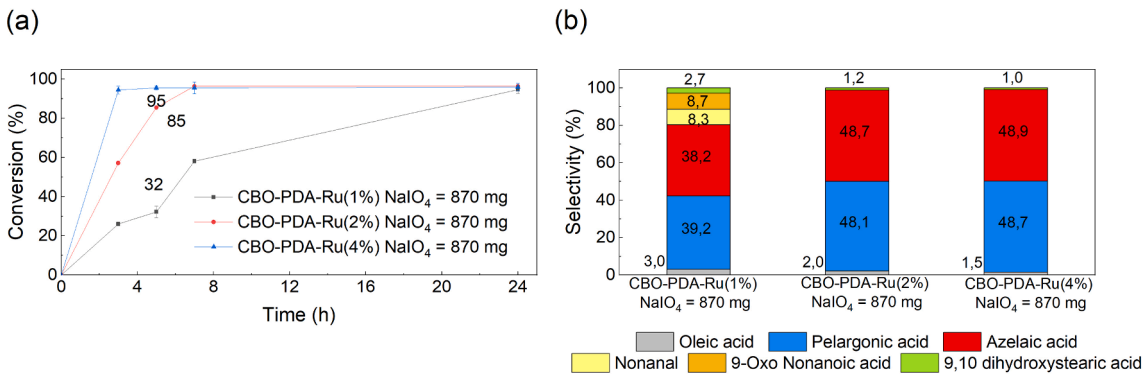

Fig. 8. a) Catalytic activity of CBO-PDA-Ru with different Ru loads at NaIO4 = 870 mg; b) Selectivity of CBO-PDA-Ru with different Ru loads.

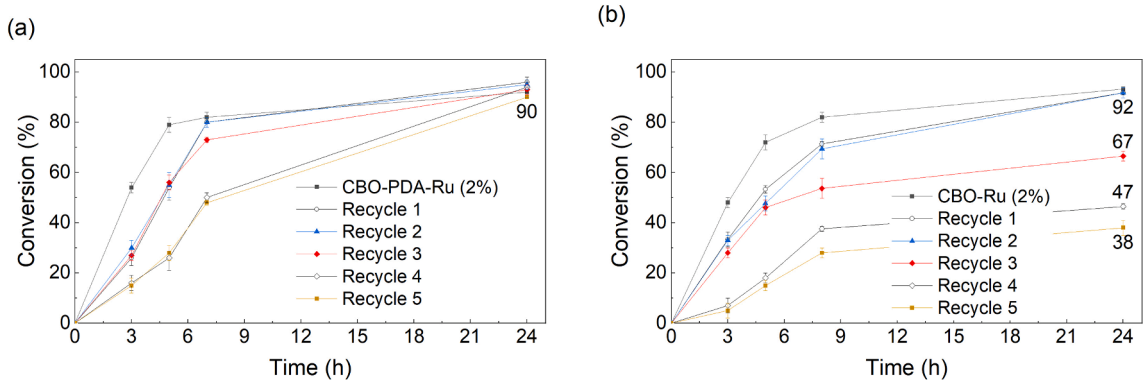

Fig. 9. Recyclability tests of: a) CBO-Ru (2%) and b) CBO-PDA-Ru (2%).

the extraction of samples for monitoring the reaction by GC. Beside this this set of experiments shows the crucial role played by PDA in the recyclability of the composite catalyst.

The results of the recyclability tests apparently contradict those from UV–Vis spectrophotometry. Indeed, on one hand the later confirmed the presence of Ru species in the reaction medium, which correspondingly should induce (as for CBO-Ru) major losses in catalytic activity along the successive recycles of CBO-PDA-Ru.

In addition, both catalysts (CBO with and without PDA) were characterized after the recycle tests. XPS analysis shows that Ru was leached after several catalytic tests in the case of CBO-Ru(2%) catalyst (Table 5). On the other hand, Ru concentration on CBO-PDA surface did not decreased during the oxidative cleavage of oleic acid. The presence of PDA was confirmed with the peak of N 1 s in the XPS spectrum of Fig. S13. The presence of Na 1 s and I 3d peaks in the spectrum of spent CBO-Ru(2%) catalyst, indicate that the composite was contaminated after several recycles (Fig. S13 c).

On the other hand, $NaIO_4$ did not contaminate CBO-PDA-Ru(2%) since Na nor I were detected by XPS. It is believed that $NaIO_4$ can oxidize PDA catechol groups; therefore, this phenomenon was verified by FTIR after fresh synthesized PDA was submitted to oxidative cleavage test. Fig. S14 shows how a small peak at 1722 cm^{-1} appears during and after the oxidation reaction [52]. This peak agrees to the stretching vibration mode of carbonyl groups, which in this case, correspond to the presence of quinones. It is possible to affirm as well that quinones are not the majority functional group of PDA chemical structure.

ICP analysis were performed as well and the results summarized in Table 6 confirm the findings observed in XPS analysis. Ru loading decreased as a consequence of several catalytic tests. The loss of Ru is higher in the case of CBO-Ru(2%) composite than in CBO-PDA-Ru(2%) catalyst. ICP and XPS results confirm that PDA functional groups allow to retain Ru on composités surface in order to maintain the catalytic activity. Ru dispersion diminished in the composite without PDA as a consequence of Ru aggregation and leaching after oxidative cleavage tests.

Clearly, the synthesized composite behaved better in the oxidative cleavage of oleic acid than CBO without PDA. In order to understand better the mechanism associated with CBO-PDA-Ru(2%) catalyst, we first evaluated in what extent the dissolved Ru in the reaction medium contributed to the oxidative cleavage of oleic acid. Therefore, a hot-

Table 5
Chemical characterization by XPS of fresh and spent catalysts.

Catalyst	C (%)	O (%)	N (%)	Ru (%)	Cl (%)	Na (%)	I (%)
Fresh CBO-Ru (2%)	89.6	8.6	—	1.8	—	—	—
Fresh CBO-PDA-Ru (2%)	68.8	21.6	7.7	1.7	0.3	—	—
Spent CBO-Ru (2%)	75.0	20.0	—	0.9	—	2.7	1.2
Spent CBO-PDA-Ru (2%)	71.3	19.3	7.6	1.6	—	—	—

Table 6
Ru loading and dispersion fresh and spent catalysts.

Catalyst	Ru loading (Nominal value) (%)	Ru loading (ICP value) (%)	Ru dispersion (%)
Fresh CBO-Ru (2%)	2.0	1.7	47.8
Fresh CBO-PDA-Ru(2%)	2.0	1.9	7.8
Spent CBO-Ru (2%)	2.0	1.1	36.1
Spent CBO-PDA-Ru(2%)	2.0	1.8	7.4

centrifugation test was performed (Fig. 10).

When conversion reached approximately 50%, the solid catalyst was removed from the reaction mixture by centrifugation. Afterwards, the reaction mixture (with-out the solid catalyst) was agitated and samples were extracted from the organic layer in order to monitor the reaction up to 24 h. Fig. 10 demonstrates that the oxidative cleavage of oleic acid proceeded after the catalyst removal with an increase of 14% in terms of conversion for CBO-Ru (2%) and 10% for CBO-PDA-Ru (2%) respectively.

This finding corroborates the understanding reached from UV–Vis spectra that a leaching occurred, since Ru species are the only capable to perform the reaction. The only way to reconciliate the facts that a leaching of active Ru species occurred, but still that the catalyst maintained the same catalytic activity after 5 recycles, is to evoke the possibility that the CBO-PDA-Ru system behaves along a boomerang catalytic mechanism.

3.3. Boomerang catalysis

This kind of catalytic system combines the benefits of heterogeneous and homogeneous catalysis [53-56]. The strategy of the boomerang catalysis consists in the development of a support that allows the release of the active species in the liquid reaction medium and once the reaction is completed, these active species should be recaptured by the support in order to re-use them in subsequent catalytic cycles [54-57]. Thereby, on one hand, it is possible to obtain the advantages of a homogenous catalyst (high catalytic activity and selectivity) and the advantages of a heterogeneous catalysts (easy separation and recycling) on the other hand [54-59].

In order to assess this possibility with our catalytic system, the protocol explained in the experimental section and depicted in Fig. 11a was performed.

After performing an oxidative cleavage test with 100 mg CBO-PDA-Ru (2%) for 24 h, the solid catalyst was re-moved by centrifugation. Therefore, initially there was 2 mg of Ru on the composite surface. Then, the organic layer was removed along with three subsequent extractions with fresh ethyl acetate in order to ensure that all the products were removed from the aqueous phase. The ICP analysis determined that 0.043 mg of Ru remained in the aqueous phase after the oxidative cleavage reaction which means a loss of Ru of 2.2% from the original catalyst. Next, a fresh support CBO-PDA was added to the aqueous layer to adsorb the leached Ru for 24 h.

The new composite CBO-PDA-(Ru recovered) adsorbed 75% of the Ru left in the aqueous layer. The catalytic test results shown in Fig. 10b confirms that the residual amount of Ru that remained in the aqueous phase after the first oxidative cleavage test was not enough to perform the oxidative cleavage of oleic acid (only 3% of conversion was reached). The composite CBO-PDA-(Ru recovered) achieved only a 14% of conversion. These findings clearly demonstrate that the synthesized composite recovered its Ru ions once the oxidative cleavage test ended since almost all Ru ions remained on its surface. These evidences explain how the composite can complete subsequent catalytic tests reaching conversions of 95% without losing catalytic activity. In addition, it is possible to affirm that the real benefit of PDA lies in its capacity to chelate Ru species after an oxidative cleavage test finishes. Thus, functional groups of the polymer may form complexes with Ru ions ("catch" of the active species) in order to "release" them in subsequent catalytic tests as a Boomerang system. The synthesized CBO-PDA-Ru composites combine the benefits of homogeneous catalysis (high catalytic activity) with those of heterogeneous catalysis (recycling of the solid catalyst). Finally, after considering all the findings shown and discussed in this section, the mechanism for the oxidative cleavage of oleic acid with CBO-PDA-Ru is illustrated in Scheme 4.

After the composite is put in contact with $NaIO_4$ in the reaction medium, Ru is released and oxidized to $Ru(VIII)O_4$. Then, a pericyclic reaction takes place between the carbon–carbon double bond of oleic acid and $Ru(VIII)O_4$ in order to form a cyclic perruthenate ester. The cyclic ester is broken by water and ruthenium is reduced to $Ru(VI)O_4$ whereas at the same time 9,10-dihydroxystearic acid is formed. $NaIO_4$ *trans*-forms the resulted diol into nonanal and 9-oxo nonanoic acid. Simultaneously, ruthenium is oxidized again to $Ru(VIII)O_4$ which in turn oxidizes the aldehydes to pelargonic and azelaic acid. It is important to remind that $NaIO_4$ can perform the latter reaction only in a minor extent. When the reaction ends, Ru is readsorbed by PDA functional groups which maintains the catalytic activity of the catalyst in subsequent reactions.

4. Conclusion

A novel Ru heterogeneous composite catalyst suitable for the oxidative cleavage of oleic acid was synthesized using carbon black as a support and polydopamine as an anchoring system for the complexation of Ru ions. The deposition of PDA on CBO surface was confirmed by FTIR, TGA, N_2 physisorption, TEM and XPS and Ru load was determined by ICP. The synthesized catalyst resulted to be active in the oxidative cleavage of oleic acid reaching conversions of 95% after 3 h of agitation at room temperature.

PDA was not detrimental for this kind of reaction and higher Ru loads increased the selectivity towards pelargonic and azelaic acid. NMR and GC analysis demonstrated the presence of intermediates such us 9,10-dihydroxystearic acid, nonanal and 9-oxo nonanoic acid. In this work, 100 mg of CBO-PDA-Ru with a Ru load of 2% along with 870 mg of $NaIO_4$ was required to transform the mentioned intermediates in the desired products.

UV–Vis analysis confirmed the presence of $Ru(VIII)O_4$ and $Ru(VI)O_4$ in the reaction medium during catalytic tests. However, once the reaction ends, the presence of Ru species was not detected anymore. On the other hand, recyclability tests demonstrated that CBO-PDA-Ru (2%)

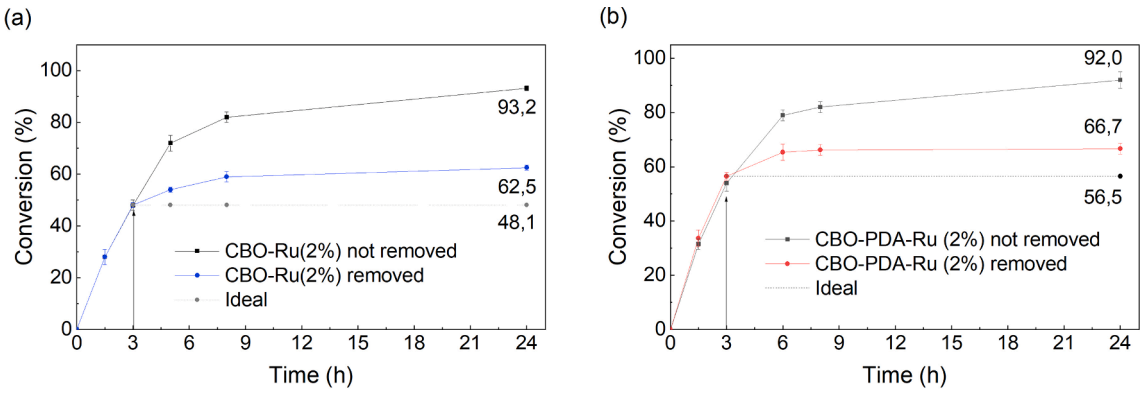

Fig. 10. Hot-filtration test results of: a) CBO-Ru (2%) and b) CBO-PDA-Ru (2%).

(a)

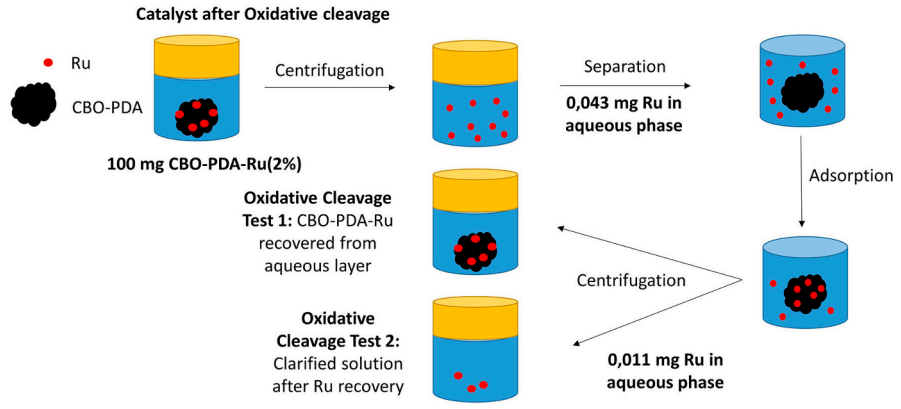

(b)

Fresh Catalyst	Catalyst after test	Aqueous phase	Fresh support after adsorption	Exhausted solution
2 mg Ru	1.95 mg Ru	0.043 mg Ru	0.032 mg Ru	0.011 mg Ru

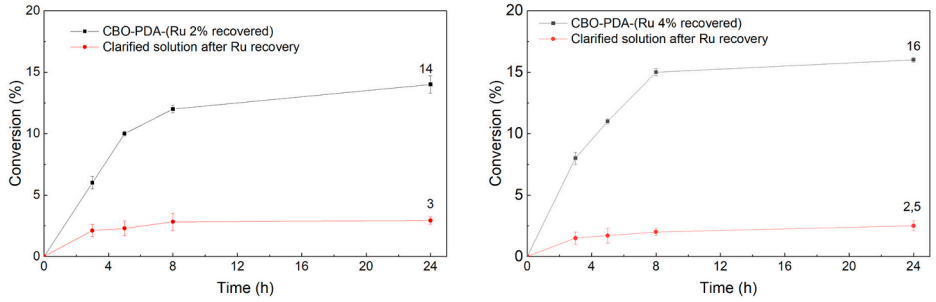

Fig. 11. a) Boomerang catalysis assessment of CBO-PDA-Ru (2%) after an oxidative cleavage test; b) Catalytic activity of CBO-PDA after adsorption of Ru within reaction media with 2% and 4% of Ru loading.

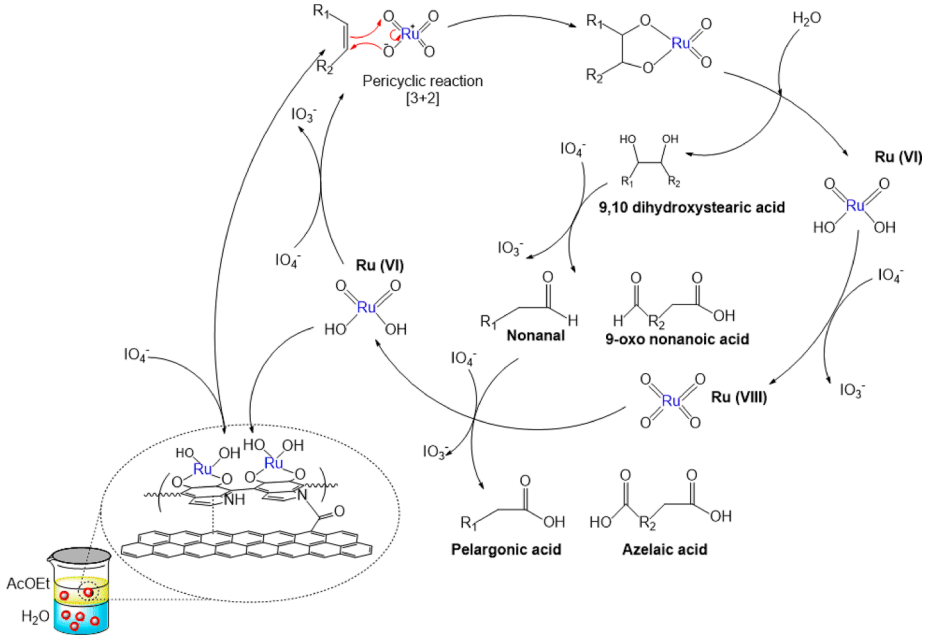

Scheme 4. Proposed mechanism for the oxidative cleavage of oleic acid with CBO-PDA-Ru.

catalyst did not lose catalytic activity even after 5 recycles. GC and ICP results confirmed that almost all Ru is recovered by PDA functional groups once the reaction ends. Hence, these findings suggest that the synthesized composite functions as a boomerang catalyst combining the advantages of homogeneous and heterogeneous catalysis in order to produce high value products from renewable raw materials like oleic acid.

Author contributions

The manuscript was written through contributions of all authors. All authors have given approval to the final version of the manuscript. Sebastián Gámez and Eric M. Gaigneaux contributed equally in the conception of the idea and the investigation carried out. Ernesto de la Torre gave supporting assistance in the development of the research.

Funding sources

“Coopération au développement” doctoral program awarded to Sebastián Gámez. The project PII-DEMEX001-2018 of the Escuela Politécnica Nacional at the initial stages of the pre-sent work.

Declaration of Competing Interest

The authors declare that they have no known competing financial interests or personal relationships that could have appeared to influence the work reported in this paper.

Acknowledgment

The authors thank the “Université catholique de Louvain” for the scholarship awarded to Sebastián Gámez in the frame of the “Coopération au développement” doctoral program. In addition, the authors address their thanks to the funding project PII-DEMEX001-2018 and of the Escuela Politécnica Nacional for the support in the initial part of the present work.

Appendix A. Supplementary data

Supplementary data to this article can be found online at https://doi.org/10.1016/j.cej.2021.131820. Catalyst characterization and reaction monitoring are included in this section.

References

[1] S. Mecking, Nature or petrochemistry?—biologically degradable materials, Angew. Chem., Int. Ed. 43 (2004) 1078–1085, https://doi.org/10.1002/anie.200301655.
[2] A. Corma Canos, S. Iborra, A. Velty, Chemical routes for the transformation of biomass into chemicals, Chem. Rev. 107 (6) (2007) 2411–2502, https://doi.org/10.1021/cr050989d.
[3] P.T. Anastas, M.M. Kirchhoff, Origins, current status, and future challenges of green chemistry, Acc. Chem. Res. 35 (9) (2002) 686–694, https://doi.org/10.1021/ar010065m.
[4] B.C. Schulte, W. Wu, T. Rosen, Azelaic Acid: Evidence-based Update on Mechanism of Action and Clinical Application, Journal of Drugs in Dermatology: JDD. 14 (9) (2015) 964–968. https://pubmed.ncbi.nlm.nih.gov/26355614/.
[5] A. Marquet. Comprehensive Natural Products II: Chapter 7.6 Biosynthesis of Biotin. Reference Module in Chemistry, Molecular Sciences and Chemical Engineering. 2010, Elsevier Science. pp. 161-180. 10.1016/B978-008045382-8.00136-2.
[6] A. Kerenkan, A. Béland, T. Do, Chemically catalyzed oxidative cleavage of unsaturated fatty acids and their derivatives into valuable products for industrial applications: a review and perspective, Catal. Sci. Technol. 6 (2016) 971–987, https://doi.org/10.1039/c5cy01118c.
[7] U. Biermann, U. Bornscheuer, M. Meier, J.O. Metzger, H. Schäfer, Oils and fats as renewable raw materials in chemistry, Angew. Chem. Int. Ed. 50 (2011) 3854–3871, https://doi.org/10.1002/anie.201002767.
[8] H. Baumann, M. Bühler, H. Fochem, F. Hirsinger, H. Zoebe-lein, J. Falbe, Natural fats and oils—renewable raw materials for the chemical industry, Angew. Chem., Int. Ed. Engl. 27 (1) (1988) 41–62, https://doi.org/10.1002/anie.198800411.
[9] K. Hill, Fats and oils as oleochemical raw materials, Pure Appl. Chem. 72 (2000) 1255–1264, https://doi.org/10.1351/pac200072071255.
[10] R. Criegee, Mechanism of ozonolysis, Angew. Chem., Int. Ed. Engl. 14 (11) (1975) 745–752, https://doi.org/10.1002/anie.197507451.
[11] R.G. Ackman, M.E. Retson, L.R. Gallay, F.A. Vandenheuvel, Ozonolysis of unsaturated fatty acids. I. Ozonolysis of oleic acid, Can. J. Chem. 39 (1961) 1956–1963, https://doi.org/10.1139/v61-262.
[12] B.R. Travis, R.S. Narayan, B. Borhan, Osmium tetroxide-promoted catalytic oxidative cleavage of olefins: an organometallic ozonolysis, J. Am. Chem. Soc. 124 (2002) 3824–3825, https://doi.org/10.1021/ja017295g.
[13] T.A. Foglia, P.A. Barr, A.J. Malloy, M.J. Costanzo, Oxidation of unsaturated fatty acids with ruthenium and osmium tetroxide, J. Am. Oil Chemists’ Soc. 54 (11) (1977), https://doi.org/10.1007/BF02909058.
[14] P. Spannring, V. Yazerski, P.C.A. Bruijnincx, B.M. Weckhuysen, R.J.M. Klein Gebbink, Fe-catalyzed one-pot oxidative cleavage of unsaturated fatty acids into aldehydes with hydrogen peroxide and sodium periodate, Chem. - A Eur. J. 19 (44) (2013) 15012–15018, https://doi.org/10.1002/chem.201301371.
[15] A. Enferadi-Kerenkan, A.S. Ello, T.O. Do, Synthesis, organo-functionalization, and catalytic properties of tungsten oxide nanoparticles as heterogeneous catalyst for oxidative cleavage of oleic acid as a model fatty acid into diacids, Ind. Eng. Chem. Res. 56 (38) (2017) 10639–10647, https://doi.org/10.1021/acs.iecr.7b03001.
[16] L.C. de La Garza, K. de Oliveira Vigier, G. Chatel, A. Moores, Amphiphilic dipyridinium-phosphotungstate as an efficient and recyclable catalyst for triphasic fatty ester epoxidation and oxidative cleavage with hydrogen peroxide, Green Chem. 19 (12) (2017) 2855–2862, https://doi.org/10.1039/c7gc00298j.
[17] S S. Warwel, M. Sojka, and M. Klaas, M. Synthesis of dicar-boxylic acids by transition-metal catalyzed oxidative cleavage of terminal-unsaturated fatty acids. In: Herrmann W.A. (eds) Organic Peroxygen Chemistry. Topics in Current Chemistry, vol 164. Springer, Berlin, Heidelberg. pp. 81-96. 10.1007/3-540-56252-4_26.
[18] S. Rup, F. Zimmermann, E. Meux, M. Schneider, M. Sindt, N. Oget, The ultrasound-assisted oxidative scission of monoenic fatty acids by ruthenium tetroxide catalysis: Influence of the mixture of solvents, Ultrason. Sonochem. 16 (2009) 266–272, https://doi.org/10.1016/j.ultsonch.2008.08.003.
[19] P. Spannring, P.C.A. Bruijnincx, B.M. Weckhuysen, R.J. Gebbink, Transition metal-catalyzed oxidative double bond cleavage of simple and bio-derived alkenes and unsaturated fatty acids, Catal. Sci. Technol. 4 (2014) 2182–2209, https://doi.org/10.1039/c3cy01095c.
[20] F. Zimmermann, E. Meux, J.L. Mieloszynski, J.M. Lecuire, N. Oget, Ruthenium catalysed oxidation without CCl_4 of oleic acid, other monoenic fatty acids and alkenes, Tetrahedron Lett. 46 (18) (2005) 3201–3203, https://doi.org/10.1016/j.tetlet.2005.03.052.
[21] H. Noureddini, M. Kanabur, Liquid-phase catalytic oxidation of unsaturated fatty acids, Journal of the American Oil Chemists’ Society 76 (3) (1999) 305–312, https://doi.org/10.1007/s11746-999-0236-7.
[22] S.E. Dapurkar, H. Kawanami, T. Yokoyama, Y. Ikushima, Catalytic oxidation of oleic acid in supercritical carbon dioxide media with molecular oxygen, Top. Catal. 52 (2009) 707–713, https://doi.org/10.1007/s11244-009-9212-6.
[23] U.S. Bäumer, H.J. Schäfer, Cleavage of olefinic double bonds by mediated anodic oxidation, Electrochim. Acta 48 (5) (2003) 489–495, https://doi.org/10.1016/S0013-4686(02)00715-6.
[24] P.H.J. Carlsen, T. Katsuki, V.S. Martin, K. Sharpless, A greatly improved procedure for ruthenium tetroxide catalyzed oxidations of organic compounds, J. Org. Chem. 46 (19) (1981) 3936–3938, https://doi.org/10.1021/jo00332a045.
[25] V.J. Shiner, C.R. Wasmuth, Kinetics and mechanism of the periodate oxidation of α-diketones, J. Am. Chem. Soc. 81 (1) (1959) 37–42, https://doi.org/10.1021/ja01510a009.
[26] C.M. Ho, W.Y. Yu, C.M. Che, Ruthenium nanoparticles supported on hydroxyapatite as an efficient and recyclable catalyst for cis-dihydroxylation and oxidative cleavage of alkenes, Angewandte Chemie - International Edition 43 (25) (2004) 3303–3307, https://doi.org/10.1002/anie.200453703.
[27] B. Lim, M. Jiang, P.H.C. Camargo, E.C. Cho, J. Tao, X. Lu, Y. Xia, Pd-Pt bimetallic nanodendrites with high activity for oxygen reduction, Science 324 (5932) (2009) 1302–1305, https://doi.org/10.1126/science.1170377.
[28] B.H.R. Suryanto, C. Zhao, Surface-oxidized carbon black as a catalyst for the water oxidation and alcohol oxidation reactions, Chem. Commun. 52 (38) (2016) 6439–6442, https://doi.org/10.1039/c6cc01319h.
[29] T. Reier, M. Oezaslan, P. Strasser, Electrocatalytic Oxygen Evolution Reaction (OER) on Ru, Ir, and Pt catalysts: a comparative study of nanoparticles and bulk materials, ACS Catal. 2 (8) (2012) 1765–1772, https://doi.org/10.1021/cs3003098.
[30] H. Liao, Y. Xiao, X. Yu, X. Liu, H. Zhong, M. Liang, H. He, Benzene hydrogenation over polydopamine-modified MCM-41 supported Ruthenium-Lanthanum catalyst, Inorganic and Nano-Metal Chemistry 48 (12) (2018) 599–606, https://doi.org/10.1080/24701556.2019.1567539.
[31] W. Froncisz, T. Sarna, J.S. Hyde, Cu^{2+} probe of metal-ion binding sites in melanin using electron paramagnetic resonance spectroscopy. I. Synthetic melanins, Arch. Biochem. Biophys. 202 (1) (1980) 289–303, https://doi.org/10.1016/0003-9861(80)90430-0.
[32] Y. Liu, K. Ai, L. Lehui, Polydopamine and its derivative materials: synthesis and promising applications in energy, environmental, and biomedical fields, Chem. Rev. 114 (2014) 5057–5115, https://doi.org/10.1021/cr400407a.
[33] C. Chen, K. Zhu, K. Chen, A. Alsaedi, T. Hayat, Synthesis of Ag nanoparticles decoration on magnetic carbonized polydopamine nanospheres for effective catalytic reduction of Cr(VI), J. Colloid Interface Sci. 526 (2018) 1–8, https://doi.org/10.1016/j.jcis.2018.04.094.
[34] N. Ghorbani, H. Namazi, Polydopamine-graphene/Ag–Pd nanocomposite as sustainable catalyst for reduction of nitrophenol compounds and dyes in

environment, Mater. Chem. Phys. 234 (2019) 38–47, https://doi.org/10.1016/j.matchemphys.2019.05.085.
[35] H. Qiao, C. Zhang, X. Dang, H. Yang, Y. Wang, Y. Chen, L. Ma, S. Han, H. Lin, X. Zhang, J. Lan, Y. Huang, Gallium loading into a polydopamine-functionalised SrTiO3 nanotube with combined osteoinductive and antimicrobial activities, Ceram. Int. 45 (17) (2019) 22183–22195, https://doi.org/10.1016/j.ceramint.2019.07.240.
[36] V. Ball, Polydopamine films and particles with catalytic activity, Catal. Today 301 (2018) 196–203, https://doi.org/10.1016/j.cattod.2017.01.031.
[37] I.D. Rosca, F. Watari, M. Uo, T. Akasaka, Oxidation of multiwalled carbon nanotubes by nitric acid, Carbon 43 (15) (2005) 3124–3131, https://doi.org/10.1016/j.carbon.2005.06.019.
[38] Q. Wei, F. Zhang, J. Li, B. Li, C. Zhao, Oxidant-induced dopaminepolymerization for multifunctional coatings, Polym. Chem. 1 (9) (2010) 1430–1433, https://doi.org/10.1039/c0py00215a.
[39] M. Ramani, B.S. Haran, R.E. White, B.N. Popov, Synthesis and characterization of hydrous ruthenium oxide-carbon supercapacitors, J. Electrochem. Soc. 148 (2001) 4, https://doi.org/10.1149/1.1357172.
[40] J. Cai, T. Chen, L. Cui, Q. Jia, M. Liu, R. Zheng, G. Yan, D. Wei, J. Liu, A three-dimensional and porous bi-nanospheres electrocatalytic system constructed by in situ generation of Ru nanoclusters inside and outside polydopamine nanoparticles for highly efficient hydrogen evolution reaction, Int. J. Hydrogen Energy 45 (11) (2020) 6592–6603, https://doi.org/10.1016/j.ijhydene.2020.01.020.
[41] V. Ball, I. Nguyen, M. Haupt, C. Oehr, C. Arnoult, V. Toniazzo, D. Ruch, The reduction of Ag+ in metallic silver on pseudomelanin films allows for antibacterial activity but does not imply unpaired electrons, J. Colloid Interface Sci. 364 (2) (2011) 359–365, https://doi.org/10.1016/j.jcis.2011.08.038.
[42] F. Rouquerol, L. Luciani, P. Llewellyn, R. Denoyel and J. Rouquerol, Texture des matériaux pulvérulents ou poreux. Téchniques de l'ingénieur, 2003, Matériaux fonctionnels, https://www.techniques-ingenieur.fr/base-documentaire/archives-th12/archives-materiaux-fonctionnels-tian0/archive-3/texture-des-materiaux-pulverulents-ou-poreux-p1050/.
[43] S.L. Goertzen, K.D. Thériault, A.M. Oickle, A.C. Tarasuk, H.A. Andreas, Standardization of the Boehm titration. Part I. CO2 expulsion and endpoint determination, Carbon 48 (4) (2010) 1252–1261, https://doi.org/10.1016/j.carbon.2009.11.050.
[44] J.P. Chen, S. Wu, Acid/Base-treated activated carbons: characterization of functional groups and metal adsorptive properties, Langmuir 20 (6) (2004) 2233–2242, https://doi.org/10.1021/la0348463.
[45] K. Hadjiivanov, J.C. Lavalley, J. Lamotte, F. Mauge, J. Saint-Just, M. Che, J. Catal. 176 (2) (1998) 415–425, https://doi.org/10.1006/jcat.1998.2038.
[46] D. Morgan, Resolving ruthenium: XPS studies of common ruthenium materials, Surf. Interface Anal. 47 (2015) 1072–1079, https://doi.org/10.1002/sia.5852.
[47] C. Pirlot, I. Willems, A. Fonseca, J.B. Nagy, J. Delhalle, Preparation and characterization of carbon nanotube/polyacrylonitrile composites, Adv. Eng. Mater. 4 (2002) 109–114, https://doi.org/10.1002/1527-2648(200203)4:3<109::AID-ADEM109>3.0.CO;2-5.
[48] J. Rojas, M. Toro-Gonzalez, M. Molina-Higgins, C. Castano, Facile radiolytic synthesis of ruthenium nanoparticles on graphene oxide and carbon nanotubes, Mater Sci Eng B 205 (2016) 28–35, https://doi.org/10.1016/j.mseb.2015.12.005.
[49] Y. Zhang, H. Jiang, G. Li, M. Zhang, Controlled synthesis of highly dispersed and nanosized Ru catalysts supported on carbonaceous materials via supercritical fluid deposition, RSC Adv 6 (2016) 16851–16858, https://doi.org/10.1039/C5RA27956A.
[50] Y. Xiang-rong, Surface and interface analysis, A mixed X-ray source for XPS and X-AES, Surf. Interface Anal. 10 (1987) 262–264, https://doi.org/10.1002/sia.740100508.
[51] C. Fernández, C. Sassoye, N. Flores, N. Escalona, E. Gaigneaux, C. Sanchez, P. Ruiz, Insights in the mechanism of deposition and growth of RuO_2 colloidal nanoparticles over alumina. Implications on the activity for ammonia synthesis, Appl. Catal. A 502 (2015) 48–56, https://doi.org/10.1016/j.apcata.2015.05.023.
[52] R.A. Zangmeister, T.A. Morris, M.J. Tarlov, Characterization of polydopamine thin films deposited at short times by autoxidation of dopamine, Langmuir 29 (27) (2013) 8619–8628, https://doi.org/10.1021/la400587j.
[53] C. Djerassi, R.R. Engle, Oxidations with ruthenium tetroxide, J. Am. Chem. Soc. 75 (15) (1953) 3838–3840, https://doi.org/10.1021/ja01111a507.
[54] M. Gruttadauria, F. Giacalone, R. Noto, "Release and catch" catalytic systems, Green Chem. 15 (2013) 2608–2618, https://doi.org/10.1039/c3gc41132j.
[55] C. Baleizão, B. Gigante, H. Garcia, A. Corma, Vanadyl salen complexes covalently anchored to single-wall carbon nanotubes as heterogeneous catalysts for the cyanosilylation of aldehydes, J. Catal. 221 (1) (2004) 77–84, https://doi.org/10.1016/j.jcat.2003.08.016.
[56] S. Kanaoka, N. Yagi, Y. Fukuyama, S. Aoshima, H. Tsuno-yama, T. Tsukuda, H. Sakurai, Thermosensitive gold nanoclusters stabilized by well-defined vinyl ether star polymers: reusable and durable catalysts for aerobic alcohol oxidation, J. Am. Chem. Soc. 129 (2007) 12060–12061, https://doi.org/10.1021/ja0735599.
[57] H. Hamamoto, Y. Suzuki, Y.M.A. Yamada, H. Tabata, H. Takahashi, S. Ikegami, A recyclable catalytic system based on a temperature-responsive catalyst, Angewandte Chemie - International Edition 44 (29) (2005) 4536–4538, https://doi.org/10.1002/anie.200500574.
[58] A. Ohtaka, Y. Tamaki, Y. Igawa, K. Egami, O. Shimomura, R. Nomura, Polyion complex stabilized palladium nanoparticles for Suzuki and Heck reaction in water, Tetrahedron 66 (30) (2010) 5642–5646, https://doi.org/10.1016/j.tet.2010.05.076.
[59] A. Ohtaka, T. Okagaki, G. Hamasaka, Y. Uozumi, T. Shinagawa, O. Shimomura, R. Nomura, Application of "boomerang" linear polystyrene-stabilized Pd nanoparticles to a series of C-C coupling reactions in water, Catalysts 5 (1) (2015) 106–118, https://doi.org/10.3390/catal5010106.